

ANGULAR DIAMETERS AND FLUXES OF MAGELLANIC CLOUD PLANETARY NEBULAE. II. HIGH-SPEED DIRECT IMAGING

P. R. WOOD, S. J. MEATHERINGHAM, AND M. A. DOPITA

Mount Stromlo and Siding Spring Observatories, Institute of Advanced Studies, Australian National University

AND

D. H. MORGAN

Royal Observatory, Edinburgh

Received 1986 December 1; accepted 1987 February 26

ABSTRACT

Images and fluxes of Magellanic Cloud planetary nebulae have been obtained with a time resolution of 1/60 s. The high time resolution was used to remove translational seeing effects and produce the sharpest possible images for the prevailing observing conditions. Angular diameters greater than 0".7 have been obtained for 20 Magellanic Cloud planetary nebulae, and fluxes in $H\beta$ or $[O III] \lambda 5007$ or both have been obtained for 80 nebulae. Masses have been derived for 18 nebulae from the angular diameters and $H\beta$ fluxes. A comparison of the masses derived here with the masses derived previously from speckle interferometry in Paper I of this series (Wood, Bessell, and Dopita 1986), and with the masses derived by Gathier *et al.* (1983) for planetary nebulae near the Galactic center, indicates that the ionized masses of typical Magellanic Cloud planetary nebulae increase with radius R roughly as $R^{3/2}$ to $R^{5/3}$ until $R \approx 0.1$ pc; thereafter, the ionized mass has a maximum value of $\sim 0.5 M_{\odot}$, a value that is predicted for the total mass of the envelope ejected by a typical precursor star in the Magellanic Clouds. Bolometric luminosities have been estimated for the central stars of those objects for which $H\beta$ fluxes were obtained. None of the planetaries has $\log L/L_{\odot} > 4.0$, again consistent with the luminosities predicted from the properties of the precursor stars.

Subject headings: galaxies: Magellanic Clouds — nebulae: planetary — stars: evolution — stars: mass loss

I. INTRODUCTION

A problem which has plagued the study of planetary nebulae (PNe) in the Galaxy is the lack of an accurate distance scale. By studying planetary nebulae in the Magellanic Clouds this problem is immediately overcome. However, another problem arises in the study of Magellanic Cloud nebulae: their diameters are typically less than $\sim 1''$ so that it is difficult to get size information for them; high spatial resolution is clearly required. In the first paper in this series (Wood, Bessell, and Dopita 1986), speckle interferometry was used to obtain angular diameters for seven nebulae. These PNe were among the brightest known in the Clouds, and they are small (angular diameters $\phi < 0".32$); it is not possible to obtain speckle diameters for faint or large objects in a reasonable time.

In the current paper, our objective is to find angular diameters for the fainter and larger ($\phi > 0".7$) nebulae using direct imaging techniques. In addition, we have used the images obtained to derive nebular line fluxes in $H\beta$ and $[O III] \lambda 5007$. Using the angular diameters and $H\beta$ line fluxes, we have derived the ionized mass in each nebula. The $H\beta$ flux can also be used to derive an approximate (accurate to better than 30%) bolometric luminosity for the central star; combined with the excitation class of Morgan (1984), this luminosity allows us to put the planetary nebula nuclei (PNNi) in an approximate H-R diagram. Finally, the masses, radii, and luminosities derived here have been compared with values expected from the study of the immediate precursor stars (the long-period variables) in the Clouds.

II. OBSERVATIONS AND DATA REDUCTION

The observations were made at the Cassegrain focus of the Anglo-Australian Telescope on the nights of 1985 October

16–17. Seeing had a full width at half-maximum (FWHM) of $\sim 1".7$ on October 16 and the second half of October 17 and a FWHM of $\sim 1".2$ during the first half of October 17. The IPCS was used as detector running in speckle mode so that the addresses of all photon events falling in each frame of duration 1/60 s were recorded. A pixel size of $0".18 \times 0".18$ and a frame size of 240×240 pixels was used, giving a total field size of $43'' \times 43''$. Narrow-band filters centered at $H\beta$ and $[O III] \lambda 5007$ were used to isolate the nebular lines.

The nebular fluxes were derived using the following procedure. Photon events recorded at each pixel were added in the usual way to make images which were subsequently divided by a normalized flat-field frame. The STARLINK program PATCH was used to remove any stars near the planetary nebula, and then the aperture photometry program in the FIGARO package was used to derive an instrumental magnitude for each object. A circular aperture of radius $3".2$ was used for most of the program objects, and the sky background was derived from a circular annulus of inner and outer radii $3".2$ and $4".2$, respectively (larger radii were used for a few of the larger PNe). Atmospheric extinction was derived by assuming an extinction coefficient of 0.11 mag per airmass. The zero-point correction to be added to the instrumental magnitudes was obtained by adopting fluxes determined previously for some of the brighter objects (Webster 1969, 1976; Osmer 1976; Aller 1983). Fluxes determined in this study are given in Table 1.

Angular diameters were determined by two methods. In the first, the radial profile of each PN image was obtained from an azimuthal average around the center of the image (the image center was obtained from program CENTRES in the FIGARO package). Then a least-squares Gaussian fit was

TABLE 1
 PLANETARY NEBULA PROPERTIES

Object ^a	Log F β ^b	Log F ₅₀₀₇ ^c	Diam(")	M/M \odot ^d	Object ^a	Log F β ^b	Log F ₅₀₀₇ ^c	Diam(")	M/M \odot ^d
LMC									
SMP 4	-13.52	-	<1.1	<0.15	SMP 9	-13.3	-12.47	<1.0	<0.16
SMP 10	-13.14	-	<1.1	<0.24	SMP 11	-13.15	-12.50	<1.0	<0.21
SMP 14	-13.68	-	1.4	0.18	SMP 15	-12.65	-	<1.0	<0.37
SMP 16	-13.29	-	0.9	0.15	SMP 18	-13.30	-	<1.1	<0.20
SMP 20	-13.42	-	<1.1	<0.17	SMP 21	-12.81	-	<1.0	<0.30
SMP 24	-13.77	-12.86	2.0	0.28	SMP 28	-13.35	-	<1.1	<0.19
SMP 30	-13.43	-12.67	<1.0	<0.15	SMP 31	-12.90	-	<1.0	<0.27
SMP 32	-12.80	-	<1.1	<0.35	SMP 35	-12.79	-	<1.1	<0.36
SMP 40	-13.44	-	<1.0	<0.15	SMP 41	-13.33	-12.19	1.5	0.31
SMP 44	-13.59	-12.54	<1.0	<0.12	SMP 45	-13.17	-	<1.0	<0.20
SMP 46	-13.60	-	<1.1	<0.14	SMP 47	-12.53	-	<1.0	<0.42
SMP 49	-13.35	-	<1.0	<0.16	SMP 50	-12.68	-	<1.0	<0.35
SMP 52	-12.53	-	<1.0	<0.42	SMP 54	-13.51	-	1.1	0.16
SMP 60	-13.63	-12.59	1.6	0.24	SMP 62	-12.32	-	<1.0	<0.53
SMP 70	-13.55	-	<1.1	<0.15	SMP 72	-13.64	-	1.6	0.24
SMP 78	-12.57	-	<1.0	<0.40	SMP 87	-12.90	-	<1.1	<0.32
SMP 95	-13.39	-	<1.1	<0.18	SMP 96	-13.34	-	<1.0	<0.16
SMP 99	-12.54	-	<1.0	<0.41	MG A0	-13.11	-	<1.0	<0.21
MG A1	-14.02	-	<1.0	<0.08	MG A4	-13.83	-12.89	0.9	0.09
MG A10	-14.02	-	<1.1	<0.09	MG A22	-13.92	-	<1.0	<0.08
MG A24	-13.56	-	<1.1	<0.15	J 4	-14.06	-13.51	3.8	0.53
J 10	-	-13.69	<1.1	-	J 12	-14.15	-13.71	1.8	0.16
J 18	-14.07	-13.37	2.5	0.28	J 20	-13.97	-13.0	1.7	0.18
J 23	-	-13.53	-	-	J 26	-	-13.21	3.2	-
SMC									
SMP 1	-12.76	-	<0.6	<0.27	SMP 2	-12.76	-	<1.0	<0.58
SMP 3	-13.07	-	<0.6	<0.19	SMP 5	-12.78	-	<0.6	<0.27
SMP 7	-13.58	-	0.8	0.16	SMP 9	-13.43	-	<0.6	<0.13
SMP 11	-12.99	-	1.0	0.45	SMP 12	-13.45	-	<0.6	<0.12
SMP 13	-12.56	-	<1.0	<0.73	SMP 14	-13.02	-12.17	<0.6	<0.20
SMP 16	-12.72	-	<1.0	<0.61	SMP 17	-12.61	-	<1.0	<0.69
SMP 18	-12.65	-	<1.0	<0.66	SMP 20	-12.47	-	<1.0	<0.82
SMP 21	-13.23	-	<1.0	<0.34	SMP 22	-12.83	-12.45	<0.6	<0.25
SMP 24	-12.69	-	<1.0	<0.63	SMP 26	-13.5	-	<1.0	<0.23
SMP 27	-12.44	-	<1.0	<0.84	J 2	-15.03	-13.52	2.3	0.15
J 6	-	-14.55	-	-	J 12	-	-13.96	<1.0	<0.00
MG 1	-14.27	-13.47	0.7	0.06	MG 2	-13.97	-13.09	1.5	0.27
MG 3	-13.63	-13.20	<0.6	<0.10	MG 4	-14.15	-	<0.6	<0.05
MG 5	-13.8	-	<0.6	<0.08	MG 6	-13.87	-13.38	<0.6	<0.08
MG 7	-13.71	-13.86	<0.6	<0.09	MG 10	-13.72	-13.55	0.7	0.10
MG 11	-14.09	-13.24	<0.6	<0.06	MG 13	-13.51	-	1.5	0.45

^a SMP numbers from Sanduleak, MacConnell, and Philip 1978; J numbers from Jacoby 1980; MG numbers in the SMC from Morgan and Good 1985; MG numbers in the LMC from Morgan and Good, private communication.

^b H β flux in ergs cm⁻² s⁻¹.

^c [O III] λ 5007 flux in ergs cm⁻² s⁻¹.

^d Mass of nebula in which hydrogen is ionized. Jacoby (1980) obtained the following angular diameters (in arcseconds): LMC J4: 3".4; LMC J10: > 1".6; LMC J12: \geq 1".3; LMC J18: > 0".6; LMC J20: \geq 2".1; LMC J26: 3".7; SMC J2: \geq 2".8.

made to the points in this profile with intensity greater than 20% of the peak intensity, and the FWHM of the observed planetary nebula image (FWHM_{IPN}) was derived from the fitted Gaussian. The same procedure was then applied to any bright point sources which occurred in the image frames so the FWHM of an observed point source image (FWHM_{IPS}) could be found. The true FWHM of the planetary nebula as estimated from the image profile (FWHM_I) was then derived from the equation (FWHM_I)² = (FWHM_{IPN})² - (FWHM_{IPS})². When there was no reasonably bright point source in the frame containing the planetary nebula, FWHM_{IPS} was obtained from a point source in a nearby (in time) frame.

The second method of deriving angular diameters was an attempt to calculate the digital autocorrelation of the instantaneous image of the object under observation. In the ideal case, this method overcomes several problems which occur with the determination of FWHM from the integrated image: image translation due to seeing effects (eliminated since the image is instantaneous), tracking errors, and errors in centering of the image. For a Gaussian image profile, the FWHM of the image is 1/(2)^{1/2} times the FWHM of the autocorrelation of the image. Full widths at half-maximum of images were obtained from the autocorrelation using this formula for both planetary nebulae (FWHM_{APN}) and point sources (FWHM_{APS}) which

occurred in the fields observed. Then a true FWHM (FWHM_A) for each planetary nebula observed was obtained from the equation $(\text{FWHM}_A)^2 = (\text{FWHM}_{\text{APN}})^2 - (\text{FWHM}_{\text{APS}})^2$. The adopted FWHM for each planetary nebula (given as the diameter in column [4] of Table 1) is the mean of FWHM_A and FWHM_I . The rms deviation of FWHM_A and FWHM_I about this mean is 11%.

In practice, the autocorrelation of the instantaneous image as required above can be obtained only approximately. If each frame is autocorrelated, two factors give an artificial spike in the center of the autocorrelation: the speckle component in the image, and the fact that each photon event is frequently spread over two (or more) adjacent pixels. To overcome these problems, the autocorrelation of each frame was approximated by the cross-correlation of each frame (i) with the following frames $i + N$ to $i + N + n$. The gap of $N - 1$ frames ($N = 16$ was used) was found to be necessary to remove the central spike in the cross-correlation resulting from either persistence in the IPCS phosphor or persistence of speckles. Each frame was cross-correlated with n frames ($n = 6$ was used in most cases) in order to increase the signal-to-noise ratio. Thus the approximate autocorrelation obtained was not instantaneous but was taken over $\sim \frac{1}{3}$ s. Tests carried out by varying N showed that, on the nights on which the observations were obtained, the FWHM of a point source increases by only 1%–2% when the autocorrelation was evaluated over $\frac{1}{3}$ s rather than over $1/60$ s. The FWHM of point sources as determined from the autocorrelation was typically 10%–20% smaller than that obtained from the integrated image.

III. DISCUSSION

a) The Ionized Mass–Radius Relation

The nebulae for which angular diameters and $\text{H}\beta$ fluxes have been determined in Papers I and II in this series are shown in the (ionized mass, nebular radius)-plane in Figure 1. Masses are derived from the formula given in Paper I. Also shown are nebulae near the Galactic center observed at radio wavelengths by Gathier *et al.* (1983). All the nebulae in Figure 1 are at well-known distances (we have assumed distances of 8.6, 52,

and 66 kpc for the Galactic center, LMC, and SMC, respectively) so that the usual problem of distance uncertainty pertaining to local Galactic planetary nebulae is overcome.

Plots similar to Figure 1 has been produced previously by Gathier *et al.* (1983) and Pottasch (1983) who argued that planetary nebulae show a large range in ionized mass, thereby making the Shklovsky method of distance determination, which assumes a constant ionized mass, very unreliable. The relations derived by Daub (1982) also imply an (ionized mass, radius)-relation similar to that in Figure 1.

It appears from Figure 1 that there is a continuous increase in ionized mass M_{ion} with nebular radius up to $R \sim 0.12$ pc; this is presumably the result of the gradual ionization of the nebula by the central star (e.g., Pottasch 1983). For these smaller nebulae, the relations $M_{\text{ion}} \propto R^{3/2}$ (Paper I) or $M_{\text{ion}} \propto R^{5/3}$ (Daub 1982) would fit equally well. The mean mass of the larger, optically thin nebulae with $R \geq 0.12$ pc is $0.27 M_{\odot}$, while the maximum mass attained by these nebulae is $\sim 0.5 M_{\odot}$. It will be assumed here that this latter mass corresponds to the total mass M_{neb} of material in the planetary nebulae in the Magellanic Clouds.

The mass M_{neb} can be related to the results obtained for other objects such as long-period variables (LPVs) in the Magellanic Clouds. The dominant population of stars currently leaving the main sequence in the LMC has an intermediate age of $\sim 2 \times 10^9$ yr (Butcher 1977; Hardy *et al.* 1984), corresponding to an initial mass of $\sim 1.6 M_{\odot}$. A similar result applies in the SMC (Hawkins and Bruck 1982; Hardy and Durand 1984). The results of the study of a complete sample of LPVs in the bar of the LMC by Wood, Bessell, and Paltoglou (1985) show that the LPV population is dominated by these intermediate-age stars. By the time they have evolved to the long-period, high-luminosity end of the LPV sequence of Wood, Bessell, and Paltoglou (1985), they have $M_{\text{bol}} \sim -5.2$, core masses of $\sim 0.65 M_{\odot}$ (from the luminosity–core mass relation for asymptotic giant branch stars [see, e.g., Wood and Zarro 1981]), present-day pulsation masses of $\sim 1.3 M_{\odot}$ (consistent with a total mass loss since the main sequence of $\sim 0.3 M_{\odot}$), and envelope masses of $\sim 0.65 M_{\odot}$ (where envelope mass is total minus core mass).

The immediate precursors of planetary nebulae in the Magellanic Clouds are the LPVs (e.g., Wood, Bessell, and Fox 1983). Since by far the most common LPVs are those of age $\sim 2 \times 10^9$ yr, it is reasonable to expect that planetary nebulae are descended predominantly from such stars also. We note that LPVs at the end of the sequence in Wood, Bessell, and Paltoglou (1985) must eject their envelopes to form planetary nebulae, as they disappear from the LPV sequence while they still have significant envelope masses ($\sim 0.65 M_{\odot}$). Given the uncertainties involved, the total planetary nebula mass of $\sim 0.5 M_{\odot}$ derived above is in good agreement with the estimate of $\sim 0.65 M_{\odot}$ for the envelope mass ejected at the end of the LPV phase.

b) Luminosities of the Central Stars

Another property of the planetary nebulae in the Magellanic Clouds which can be compared with observations of the precursor LPVs and with theory is the luminosity distribution of the central stars. Given the $\text{H}\beta$ fluxes for the nebulae from Table 1, an estimate of the bolometric luminosity of the central star can be made by assuming that each photon emitted by the central star shortward of the Lyman limit leads to one photoionization and subsequent case B recombination of a hydro-

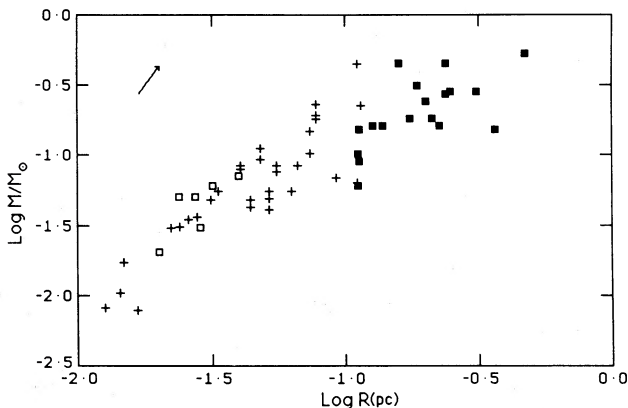


FIG. 1.—The mass M of ionized gas in planetary nebulae plotted against the nebular radius. *Filled squares*: planetary nebulae in the Magellanic Clouds for which angular diameters have been determined in this paper; *open squares*: nebulae for which angular diameters were determined in Paper I; *crosses*: nebulae near the Galactic center studied by Gathier *et al.* (1983). Distances of 8.6, 52, and 66 kpc have been assumed for the Galactic center, the LMC, and the SMC, respectively. The arrow shows the effect of a 20% increase in assumed distance.

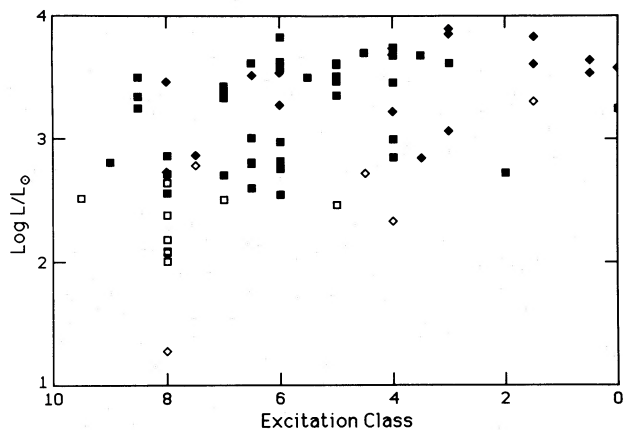


FIG. 2.—Luminosities of planetary nebula nuclei in the Magellanic Clouds plotted against the nebula excitation class from Morgan (1984). Squares: nebulae in the LMC; diamonds: nebulae in the SMC; open symbols: objects for which the radii are known to be greater than 0.12 pc.

gen atom in a gas with $T = 10^4$ K. In deriving the luminosities in Figure 2, the central star is assumed to radiate like a blackbody with a temperature of $\log T = 5.2$, corresponding to the maximum temperature reached by a planetary nebula nucleus of mass $\sim 0.65 M_{\odot}$. The number of ionizing photons per unit stellar luminosity does not vary by more than 30% from the adopted value for temperatures in the wide range $4.6 < \log T < 5.2$; thus errors in $\log L/L_{\odot}$ from this source are less than or equal to 0.15.

The luminosities of the central stars deduced in this fashion are shown plotted against excitation class (a rough measure of the temperature of the central star, but also dependent on the flux of ionizing photons per nebular atom) in Figure 2. The excitation class is obtained from Morgan (1984); when Morgan gives only a range in excitation class, the mean of the range is

used. A few additional objects are plotted in Figure 2 using the $H\beta$ fluxes given in the papers cited above as sources of standard fluxes. We note that the luminosity estimates in Figure 2 are effectively lower limits: escape of ionizing photons from the nebula (because the nebula is optically thin or because it does not completely surround the central star as in the case in bipolar nebulae) or absorption by dust in the nebula will all lead to a reduction in the luminosity estimated for the central star. Reddenings E_{B-V} to the SMC and LMC of 0.02 and 0.06 mag, respectively, have been assumed.

The largest luminosities derived for Magellanic Cloud planetary nebula nuclei are $\log L/L_{\odot} \sim 3.9$ ($M_{\text{bol}} \sim -5$), in quite good agreement with the luminosities of the dominant population of LPVs at the end of their AGB evolution. Since evolution from the asymptotic giant branch to the planetary nebula region of the H-R diagram occurs at constant luminosity, this is as expected. As planetary nebulae age, their luminosities finally decline below the peak values on the horizontal portion of the evolutionary track. The large range in luminosities exhibited in Figure 2 is probably partly due to errors in the luminosity estimates as well as to real evolutionary effects. Some further comparison of the evolution of the Magellanic Cloud planetary nebulae with theoretical evolutionary calculations is given in Wood (1986).

IV. SUMMARY

Line fluxes in $H\beta$ and $[O III] \lambda 5007$ have been obtained for a large number of planetary nebulae in the Magellanic Clouds, and angular diameters $> 0''.7$ have been derived for a smaller number of the nebulae. Ionized masses for the nebulae and luminosities for the central stars have been derived; these quantities have been shown to be in good agreement with the values expected from the properties of the immediate precursor stars, the long-period variables.

REFERENCES

- Aller, L. H. 1983, *Ap. J.*, **273**, 590.
 Butcher, H. R. 1977, *Ap. J.*, **216**, 372.
 Daub, C. T. 1982, *Ap. J.*, **260**, 612.
 Gathier, R., Pottasch, S. R., Goss, W. M., and van Gorkom, J. M. 1983, *Astr. Ap.*, **128**, 325.
 Hardy, E., Buonanno, R., Corsi, C. E., Janes, K. A., and Schommer, R. A. 1984, *Ap. J.*, **278**, 592.
 Hardy, E., and Durand, D. 1984, *Ap. J.*, **279**, 567.
 Hawkins, M. R. S., and Bruck, M. T. 1982, *M.N.R.A.S.*, **198**, 935.
 Jacoby, G. H. 1980, *Ap. J. Suppl.*, **42**, 1.
 Morgan, D. H. 1984, *M.N.R.A.S.*, **208**, 633.
 Morgan, D. H., and Good, A. R. 1985, *M.N.R.A.S.*, **213**, 491.
 Osmer, P. S. 1976, *Ap. J.*, **203**, 352.
 Pottasch, S. R. 1983, in *IAU Symposium 103, Planetary Nebulae*, ed. D. R. Flower (Reidel: Dordrecht), p. 391.
 Sanduleak, N., MacConnell, D. J., and Philip, A. G. D. 1978, *Pub. A.S.P.*, **90**, 621.
 Webster, B. L. 1969, *M.N.R.A.S.*, **143**, 79.
 ———. 1976, *M.N.R.A.S.*, **174**, 513.
 Wood, P. R. 1986, in *Workshop on the Late Stages of Stellar Evolution*, ed. S. Kwok and S. Pottasch (Dordrecht: Reidel), in press.
 Wood, P. R., Bessell, M. S., and Dopita, M. A. 1986, *Ap. J.*, **311**, 632 (Paper 1).
 Wood, P. R., Bessell, M. S., and Fox, M. W. 1983, *Ap. J.*, **272**, 99.
 Wood, P. R., Bessell, M. S., and Paltoglou, G. 1985, *Ap. J.*, **290**, 477.
 Wood, P. R., and Zarro, D. M. 1981, *Ap. J.*, **247**, 247.

M. A. DOPITA, S. J. MEATHERINGHAM, and P. R. WOOD: Mount Stromlo and Siding Spring Observatories, Private Bag, Woden P.O., A.C.T. 2606, Australia

D. H. MORGAN: Royal Observatory, Blackford Hill, Edinburgh EH9 3HJ, Scotland, UK